Available online at www.sciencedirect.com
ScienceDirect
Acta Materialia 55 (2007) 6472–6480
Acta MATERIALIA
www.elsevier.com/locate/actamat

A constrained domain-switching model for polycrystalline ferroelectric ceramics. Part I: Model formulation and application to tetragonal materials

F.X. Li, R.K.N.D. Rajapakse *

Department of Mechanical Engineering, The University of British Columbia, 6250 Applied Science Lane, Vancouver, Canada V6T 1Z4

Received 24 July 2007; accepted 5 August 2007
Available online 24 September 2007

Abstract

A micromechanical model is proposed to study the constrained domain-switching process in polycrystalline ferroelectric ceramics. It is assumed that the depolarization field induced by domain switching is completely compensated by free charges, while the stress caused by non-180° switching is considered in an Eshelby inclusion manner. The model assumes that each grain contains multi-domains and the domain-switching criterion is based on potential energy density. Two switching options, which are based on Hwang et al. [Hwang SC, Lynch CS, McMeeking RM. Acta Metall Mater 1995;43:2073] and Berlincourt and Krueger [Berlincourt D, Krueger HHA. J Appl Phys 1959;30:1804], are used in the model development. Details of the switching process are analyzed for tetragonal ferroelectric/ferroelastic ceramics under electric loading or uniaxial compression (tension) by using an inverse-pole-figure method. Numerical results show that during electric poling, only a few per cent 90° switching can occur in $BaTiO_3$ ceramics, which agrees well with experimental observations.

Keywords: Charge screening; Constitutive modeling; Domain switching; Ferroelectric ceramics; Poling

1. Introduction

Perovskite ferroelectric ceramics such as barium titanate ($BaTiO_3$) and lead titanate zirconate (PZT) are commonly used to make actuators, transducers, etc., due to their electromechanical coupling, ultra-fast response and compact size [1]. This class of materials shows excellent linear response at low electric fields but under a large electric field or high stress significant nonlinearities in response occur due to domain switching [2]. Domain switching in ferroelectric ceramics is crystal symmetry related. Only 180° and 90° domain switching exists in tetragonal ceramics, and 180°, 109° and 71° switching in rhombohedral ceramics. In ferroelectric single crystals, perfect alignment of polarization can be achieved and a single domain state can exist after poling by a strong DC field. However, this is not the case in ferroelectric ceramics, where the crystallite axes arrange in a random way and multiple domain states could exist after poling. The theoretical achievable polarization and strain in perovskite ferroelectric ceramics under electric or mechanical poling have been obtained analytically [3–5] and numerically [6,7]. However, strain measurements and X-ray diffraction studies show that after poling the fraction of completed 90° switching is 10-12% in $BaTiO_3$ ceramics [8,9] and 44–51% in tetragonal PZT and lead magnesium niobate titanate (PMN-PT) ceramics near the morphotropic phase boundary (MPB) [8,10]. This implies that a considerable amount of 90° switching is constrained by neighboring grains.

Modeling of domain switching in ferroelectric materials has received much attention, and both phenomenological models [11,12] and micromechanical models [13–18] exist in the literature. In the latter models, the material usually consists of numerous grains, each of which is a single domain or contains multi-domains [15,18]. Domain

* Corresponding author. Tel.: +1 604 827 4483; fax: +1 604 822 2403.
E-mail address: rajapakse@mech.ubc.ca (R.K.N.D. Rajapakse).

1359-6454/$30.00
doi:10.1016/j.actamat.2007.08.002

switching is then determined by an energy-based switching criterion, with intergranular interactions either neglected [13] or taken into account in an Eshelby inclusion manner [14–16] or by finite element methods [17,18]. According to the authors' knowledge, only Wan and Bowman [19] have specifically addressed the fraction of 90° switching (or non-180° switching) in domain switching modeling by assuming that the depolarization field is proportional to the fraction of completed 90° switching. Although the above-mentioned domain-switching models assume that the material is purely tetragonal, most experimental results of PZT ceramics are near the MPB where tetragonal and rhombohedral phases coexist. Recently, Li et al. [20] showed through a rigorous mathematical analysis that unless caused by a very large internal stress, no change of remnant strain is generated in a polycrystalline tetragonal or rhombohedral ferroelectric ceramic via non-180° domain switching. On the other hand, in PZT ceramics near the MPB, non-180° switching can almost be achieved similar to the case of a single crystal. Li et al.'s [20] analysis can accurately interpret most experimental results except the case of rhombohedral ceramics during electric poling where considerable remnant strain by 71° or 109° domain switching has been observed [21,22].

In this paper, a micromechanical model is developed to study the constrained domain-switching phenomenon in ferroelectric/ferroelastic ceramics with grains containing multiple domains by using two previously reported polarization-switching models, i.e. Hwang et al.'s model [13] and Berlincourt and Krueger's definition of complete 180° switching [10]. A description of the proposed constrained domain-switching model is presented in Section 2. In Sections 3 and 4, the domain-switching processes in tetragonal ferroelectric and ferroelastic polycrystalline materials are analyzed in detail under electric loading and uniaxial compression (tension) by using an inverse-pole-figure method. A discussion is presented in Section 5 and the conclusions are given in Section 6. In a subsequent paper [23], a combined switching assumption is presented and used to study constrained domain switching in rhombohedral materials.

2. Constrained domain-switching model

Assume that a polycrystalline ferroelectric ceramic is made up of numerous randomly oriented grains, each of which contains N types of domains, where $N = 6$ for the tetragonal case and $N = 8$ for the rhombohedral case. In an unpoled ceramic, the fraction of each type of domain in a grain is $1/N$, thus both the remnant polarization and strain of each grain is zero. The present model is also based on the assumptions that a polycrystalline ferroelectric ceramic is dielectrically and elastically isotropic and shows linear dielectric and elastic behavior unless domain switching occurs (i.e. all nonlinear polarization and strain are caused by domain switching).

2.1. Charge-screening effect and internal stress by non-180° domain switching

The charge-screening effect in real ceramics [21,22,24] is taken into account in the proposed model. That is, the depolarization field induced by polarization gradient or polarization change during domain switching is completely compensated by free charges. The free charges are trapped by unbalanced polarization and turn in to space charges, which cannot be driven by the applied electric field unless the polarization switches. When domain switching occurs, the space charges are released and move to the surface of a material. In fact, this is the principle that is used to measure the electric hysteresis loops in the Sawyer–Tower circuit and mechanical depolarization in short circuits. The remnant polarization of a ferroelectric ceramic cannot be measured if there is no charge-screening effect. However, the depolarization field may not be completely compensated and it can be very large within a thin layer just below the crystal surface [25]; this is called the Lehovec effect [9,26,27]. This large electric field tends to orient the ferroelectric axis in the thin layer perpendicular to the surface and make domain switching more difficult than that inside a crystal [9,28]. The Lehovec effect is neglected in the present study and the present model is suitable only for bulk materials.

The internal stress induced by spontaneous strain change during non-180° domain switching cannot be compensated in a manner similar to the unbalanced polarization. The spontaneous strain change by non-180° switching is similar to the plastic strain in ductile materials [20]. According to the Taylor rule of plasticity [29], a crystal must have at least five slip systems for a polycrystalline to be ductile. In terms of the deformation modes, a ferroelectric crystal is similar to a ferroelastic crystal or a shape memory alloy [30] which has two independent slip systems for the tetragonal case and three for the rhombohedral case. Thus in tetragonal or rhombohedral polycrystalline ferroelectric ceramics, non-180° domain switching generates large internal stresses because of the spontaneous strain change during switching, i.e. such switching could be constrained by neighboring grains and may not occur. However, in orthorhombic ferroelectric ceramics or PZT ceramics near the MPB, where tetragonal and rhombohedral phases coexist, there are five or more independent deformation modes, which render the material ductile. In this case, non-180° domain switching does not generate very large internal stresses from neighboring grains and can be almost completely accomplished [20,30]. The present model excludes these "ductile" polycrystallines and focuses only on the constrained domain-switching phenomenon in tetragonal and rhombohedral ferroelectric ceramics.

Following Hwang et al. [14] and Huber et al. [15], the internal stress induced by non-180° domain switching in tetragonal and rhombohedral ceramics is considered in an Eshelby inclusion manner [31]. For simplicity, each

grain in a polycrystalline ceramic is treated as a spherical Eshelby inclusion in an infinite elastic matrix. Domain switching is assumed a quasi-static process and the strain induced by non-180° switching is averaged over the whole grain. Thus inside a grain, both the strain and internal stress are considered uniform. Under these assumptions, 180° switching is not constrained and non-180° switching is constrained by neighboring grains but not by neighboring domains.

Consider a ferroelectric ceramic with a single crystal having M types of deformation modes or ferroelastic domains ($M = 3$ for tetragonal and $M = 4$ for rhombohedral). The remnant strain in an unpoled ceramic is zero as the fraction of each type of ferroelastic domain is $1/M$. It is reasonable to assume that the unpoled state is internally stress free because of energy minimization during cooling [20]. Then, during subsequent electric or mechanical loading, the remnant strain in a grain can be expressed as:

$$\varepsilon^{\mathrm{r}} = \sum_{i=1}^{M} f_i \varepsilon^{(i)}, \tag{1}$$

where ε^{r} is the remnant strain of the whole grain, and f_i and $\varepsilon^{(i)}$ are the volume fraction and spontaneous strain of the ith ferroelastic domain in the grain, respectively.

As domain switching is a volume-conserving process, the remnant strain is a deviator tensor. The internal stress induced by domain switching can then be expressed as [31,32]:

$$\sigma_{ij}^{\mathrm{in}} = -2\mu \frac{7-5v}{15(1-v)} \varepsilon_{ij}^{\mathrm{r}}, \tag{2}$$

where μ is the shear modulus of the ceramic and v is Poisson's ratio.

The electric and stress field in a grain is obtained from the superposition of the internal field and the applied field as:

$$E_i = E_i^{\mathrm{app}}, \quad \sigma_{ij} = \sigma_{ij}^{\mathrm{app}} + \sigma_{ij}^{\mathrm{in}}, \tag{3}$$

where E_i^{app} and $\sigma_{ij}^{\mathrm{app}}$ are elements of the applied electric field and the applied stress, respectively.

2.2. Energy-based domain-switching criterion

In this section, the energy-based domain-switching criterion of Hwang et al. [13] is summarized in the context of the present model. Following Hwang et al. [13], the potential energy per unit volume of a single domain can be expressed as:

$$U = -(\boldsymbol{\sigma} : \boldsymbol{\varepsilon}^{\mathrm{s}} + \mathbf{P}^{\mathrm{s}} \cdot \mathbf{E}), \tag{4}$$

where $\mathbf{P}^{\mathrm{s}}$ and $\boldsymbol{\varepsilon}^{\mathrm{s}}$ are spontaneous polarization and strain of a specific domain, respectively, and $\mathbf{E}$ and $\boldsymbol{\sigma}$ are the electric field and stress in the domain as given by Eq. (3).

It is assumed that domain switching is driven by a change in potential energy of a domain. As 180° domain switching is not constrained because of the charge-screening effect, the switching criterion is thus identical to Hwang et al.'s model [13], i.e.:

$$U^{\mathrm{aft}} - U^{\mathrm{bef}} \geqslant W_{180}, \tag{5}$$

where U^{bef} and U^{aft} denote potential energy per unit volume before and after 180° domain switching; W_{180} is the 180° switching barrier and is equal to $2P_0E_{\mathrm{C}}$ (where P_0 is the spontaneous polarization, E_{C} the coercive field) [13–18].

Complete unconstrained 180° switching is obtained once Eq. (5) is satisfied. As non-180° domain switching is constrained by neighboring grains and the internal stress is dependent on domain fractions, the switching criterion is also domain-fraction dependent. Thus unlike 180° domain switching, non-180° switching takes place gradually as the applied field increases. A uniform non-180° domain-switching criterion for ferroelectric ceramics is not attempted here, as it is too complex. The 90° domain-switching criteria for tetragonal ferroelectric and ferroelastic polycrystalline ceramics are presented in Sections 3 and 4, respectively.

3. Constrained domain-switching model for tetragonal ferroelectric ceramics

3.1. Model formulation

A tetragonal ferroelectric crystal has six allowable polarization directions and three elongation directions. The six types of domains are defined in terms of the crystallite coordinates (x,y,z) as shown in Fig. 1 without loss of any generality. Let $\mathbf{P}^{(i)}$ and $\boldsymbol{\varepsilon}^{(i)}$ denote the spontaneous polarization vector and spontaneous strain tensor of the ith domain, respectively. Then,

$$\begin{aligned} &\mathbf{P}^{(1)} = -\mathbf{P}^{(2)} = P_0(0,0,1)^{\mathrm{T}}, \\ &\mathbf{P}^{(3)} = -\mathbf{P}^{(4)} = P_0(1,0,0)^{\mathrm{T}}, \\ &\mathbf{P}^{(5)} = -\mathbf{P}^{(6)} = P_0(0,1,0)^{\mathrm{T}} \end{aligned} \tag{6}$$

$$\boldsymbol{\varepsilon}^{(1)} = \boldsymbol{\varepsilon}^{(2)} = \frac{S_0}{3}\begin{bmatrix} -1 & & \\ & -1 & \\ & & 2 \end{bmatrix}, \quad \boldsymbol{\varepsilon}^{(3)} = \boldsymbol{\varepsilon}^{(4)} = \frac{S_0}{3}\begin{bmatrix} 2 & & \\ & -1 & \\ & & -1 \end{bmatrix}, \quad \boldsymbol{\varepsilon}^{(5)} = \boldsymbol{\varepsilon}^{(6)} = \frac{S_0}{3}\begin{bmatrix} -1 & & \\ & 2 & \\ & & -1 \end{bmatrix}, \tag{7}$$

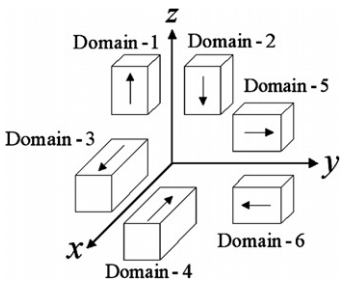

Fig. 1. Illustration of six types of domain in crystallite coordinates of tetragonal ferroelectric crystals.

where P_0 is the spontaneous polarization, S_0 is the single crystal deformation [2] or lattice deformation in tetragonal crystals ($S_0 = c/a - 1$), and c and a are the tetragonal lattice constants.

The crystal axes are randomly distributed in a polycrystalline ferroelectric ceramic. In the case of electric loading or uniaxial compression (tension), as far as the polarization and strains are concerned, it is equivalent to fix the crystallite coordinates (x, y, z) along the reference coordinates (X_1, X_2, X_3) and make the applied field direction vary [4,5] (see Fig. 2). The original condition of a random distribution of grains now means that the applied field direction distributes equally in all directions. This method is similar to the definition of the inverse pole figure in texture analysis [33] and is referred to hereafter as the inverse-pole-figure method. Because of symmetry, it is necessary only to consider the case when the applied field directions distribute in the shaded area shown in Fig. 2, which is 1/48 of the surface area of a unit sphere. The boundary curves of this area can be expressed by the Eulerian angles θ and φ, with $\varphi = 0$, $\varphi = \pi/4$ and $\cos\varphi = \cot\theta$.

Consider a grain with an electric field applied at angles (θ, φ) as shown in Fig. 2. According to the switching model of Hwang et al. [13], domain 1 is the most energetically favorable state during electric poling along the positive z-axis and there can be possible 90° switching from domains 4, 6, 3, 5 to domain 1, and possible 180° switching from domain 2 to domain 1, domain 4 to domain 3, and domain 6 to domain 5. For simplicity, "switching $i-j$" hereafter means switching from domain i to domain j. According to Berlincourt and Krueger's definition of complete 180° switching [8], the only possible 180° switching is from domain 2 to domain 1, i.e. there is no possible 180° switching from domain 4 to domain 3 or from domain 6 to domain 5. The 90° switching options of Berlincourt and Krueger [8] are identical to those of Hwang et al. [13]. In the present study, switching of individual domains is based on potential energy density using either Hwang et al.'s [13] or Berlincourt and Krueger's [8] switching options. The only difference between the two switching options is whether the 180° switchings 4-3 and 6-5 are allowed. For convenience, the constrained domain-switching models based on Hwang et al.'s [13] and Berlincourt and Krueger's [8] switching options are hereafter identified as Models A and B, respectively. The definition of complete 180° switching under Model A is thus quite different from that under Model B. For Model A, as shown in Fig. 3a, complete 180° switching means that all domains with an original polar direction that makes an obtuse angle with the electric field undergo 180° switching. While for Model B, as shown in Fig. 3b, complete 180° switching only covers those domains with an original polar direction that makes an angle of $[3\pi/4, \pi]$, and for some domains $[\pi/2 + 35.3^0, 3\pi/4]$, to the electric field [5,8].

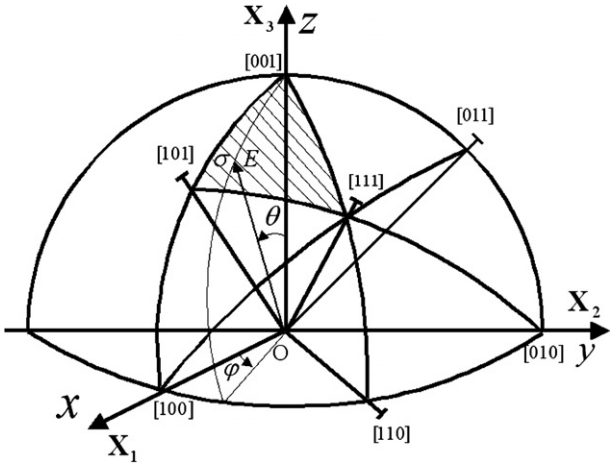

Fig. 2. Representative distribution areas of applied field in tetragonal ceramics under electric loading or uniaxial compression (tension) with the crystallite coordinates (x, y, z) fixed along the sample coordinates (X_1, X_2, X_3).

Now consider the 90° switching 4-1 as an example to establish a 90° switching criterion for a grain with multiple domains. Consider a specific domain state with domain fractions f_i $(i = 1, 2, \ldots, 6)$ and the internal stress by domain orientation can be obtained using Eqs. (1) and (2) as:

$$\sigma_{ij}^{\text{in}} = -2\mu\frac{7-5v}{15(1-v)}\left[(f_1+f_2)\varepsilon_{ij}^{(1)} + (f_3+f_4)\varepsilon_{ij}^{(3)} + (f_5+f_6)\varepsilon_{ij}^{(5)}\right]. \tag{8}$$

As the unpoled state is assumed to be free of internal stress with zero remnant strain, the internal stress of any domain orientation state can be expressed by fractions of 90° switching only. Let f_{i-j} denote the fraction of switched domains from domain i to domain j with respect to the unpoled state and $\boldsymbol{\varepsilon}^{(i-j)}$ denote the strain change during switching $i-j$. Then $\boldsymbol{\varepsilon}^{(i-j)}$ can be expressed as:

$$\boldsymbol{\varepsilon}^{(i-j)} = \boldsymbol{\varepsilon}^{(j)} - \boldsymbol{\varepsilon}^{(i)}, \tag{9}$$

and Eq. (8) can be simplified as:

$$\sigma_{ij}^{\text{in}} = -2\mu\frac{7-5v}{15(1-v)}\left[(f_{3\text{-}1}+f_{4\text{-}1})\varepsilon_{ij}^{(3\text{-}1)} + (f_{5\text{-}1}+f_{6\text{-}1})\varepsilon_{ij}^{(5\text{-}1)}\right]. \tag{10}$$

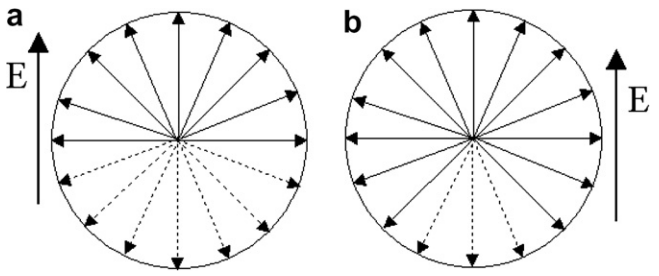

Fig. 3. Two-dimensional illustration of complete 180° switching under (a) Model A and (b) Model B. (Broken arrows denote the original polar directions of those domains which experienced 180° switching).

Now consider the 90° switching of a small fraction, Δf_{4-1}, with the electric field E applied at angles (θ, φ) as shown in Fig. 2. Using Eqs. (4), (9) and (10), the 90° switching criterion can be written as:

$$\Delta f_{4\text{-}1}\left\{(EP_0\cos\theta + EP_0\sin\theta\cos\varphi) - 2\mu\frac{7-5v}{15(1-v)}S_0^2 \right. \\ \left.[2(f_{4\text{-}1}+f_{3\text{-}1}) + \Delta f_{4\text{-}1} + f_{6\text{-}1} + f_{5\text{-}1}]\right\} \geqslant \Delta f_{4\text{-}1}\cdot W_{90}^{\mathrm{E}}, \quad (11)$$

where W_{90}^{E} is the energy barrier (per unit volume) for 90° switching under electric loading.

Following Huber et al. [15], $W_{90}^{\mathrm{E}} = W_{180}/\sqrt{2} = \sqrt{2}P_0E_{\mathrm{C}}$ to activate both 90° switching and 180° switching when the applied field reaches E. By neglecting the high-order infinitesimal terms and noting that f_{4-1} increases continuously with the applied field E, the inequality (11) can be converted to the following equation:

$$EP_0\cos\theta + EP_0\sin\theta\cos\varphi - 2\mu\frac{7-5v}{15(1-v)}S_0^2 \\ [2(f_{4\text{-}1}+f_{3\text{-}1}) + f_{6\text{-}1} + f_{5\text{-}1}] = \sqrt{2}P_0E_{\mathrm{C}}. \quad (12)$$

Divide both sides of Eq. (12) by P_0 and express the Cartesian coordinates in terms of spherical coordinates of a unit sphere, i.e.

$$x = \sin\theta\cos\varphi, \quad y = \sin\theta\sin\varphi, \quad z = \cos\theta \quad (x, y, z \geqslant 0). \quad (13)$$

Then,

$$E(z+x) - E_{\mathrm{b}}[2(f_{4\text{-}1}+f_{3\text{-}1}) + f_{6\text{-}1} + f_{5\text{-}1}] = \sqrt{2}E_{\mathrm{C}}, \quad (14)$$

where $E_{\mathrm{b}} = 2\mu\frac{7-5v}{15(1-v)}S_0^2/P_0$ is an equivalent resisting electric field induced by 90° switching.

The physical meaning of E_{b} is quite obvious. In the case where the applied field direction coincides with the X_3 axis, i.e. $\theta = 0$, when no 90° switching is accomplished, i.e. $f_{i-1} = 0$ $(i = 3, 4, 5, 6)$, the activation field for the initial 90° switching is $\sqrt{2}E_{\mathrm{C}}$. When all possible 90° switchings are nearly complete, i.e. $f_{i-1} = (1/6)^-$ $(i = 3, 4, 5, 6)$, the critical field for the last infinitesimal fraction of 90° switching is $\sqrt{2}E_{\mathrm{C}} + E_{\mathrm{b}}$. Thus, similar to the back stress in phenomenological theories of plasticity for materials experiencing the Bauschinger effect [34], E_{b} can also be called the "back electric field" induced by 90° switching.

Similarly, the criterion for the switching 3-1 is:

$$E(z-x) - E_{\mathrm{b}}[2(f_{4\text{-}1}+f_{3\text{-}1}) + f_{6\text{-}1} + f_{5\text{-}1}] = \sqrt{2}E_{\mathrm{C}} \quad (15)$$

and for the switching 6-1 and 5-1:

$$E(z \pm y) - E_{\mathrm{b}}[(f_{4\text{-}1}+f_{3\text{-}1}) + 2(f_{6\text{-}1}+f_{5\text{-}1})] = \sqrt{2}E_{\mathrm{C}}. \quad (16a, b)$$

Bearing in mind that for the shaded area in Fig. 2, $z \geqslant x \geqslant y$, it can be concluded from Eqs. (14)–(16) that switching 4-1 activates at a lower field than switching 6-1, and switching 4-1 is superior to switching 3-1, as well as switching 6-1 to switching 5-1. Switchings 3-1 and 5-1 do not activate unless switchings 4-1 and 6-1 saturate. Thus using Eqs. (14)–(16), the fraction of 90° switching can be explicitly expressed as a function of the applied electric field E and Eulerian angles (θ, φ).

Next, the detailed domain-switching process in a specific grain is considered using both Model A and Model B. First consider the case of an increasing and then vanishing electric field applied at angles (θ, φ). Note that the magnitudes of the applied electric field and stress considered in this paper are such that linear dielectric and elastic assumptions hold true.

3.1.1. Model A

First, consider the case of increasing electric loading. The unconstrained 180° switching is well established and need not to be discussed here in detail. With respect to 90° domain switching during electric poling, the switching 4-1 activates first when the electric field increases. In the cases where switchings 4-1 and 6-1 coexist, the switching criteria are:

$$\begin{cases} E(z+x) - E_{\mathrm{b}}\cdot(2f_{4\text{-}1}+f_{6\text{-}1}) = \sqrt{2}E_{\mathrm{C}} \\ E(z+y) - E_{\mathrm{b}}\cdot(f_{4\text{-}1}+2f_{6\text{-}1}) = \sqrt{2}E_{\mathrm{C}} \end{cases} \quad (17a, b)$$

The fractions of switchings 4-1 and 6-1 can be obtained by solving Eqs. (17a) and (17b) as:

$$\begin{cases} f_{4\text{-}1} \\ f_{6\text{-}1} \end{cases} = \min\left\{\frac{E(2z+x+y) - 2\sqrt{2}E_{\mathrm{C}}}{6E_{\mathrm{b}}} \pm \frac{E}{2E_{\mathrm{b}}}(x-y), 1/6\right\}. \quad (18)$$

In the cases where only one type of 90° switching exists, the analysis is well established and is not presented here. As mentioned before, switchings 3-1 and 5-1 do not activate before f_{4-1} and f_{6-1} saturate. Note that under Model A, once the switching condition for 180° switching 4-3 (or 6-5) is satisfied, 90° switching 4-1 (or 6-1) ceases.

The switching-induced polarization and strain can be obtained by integration over the shaded surface areas shown in Fig. 2. Note that in this paper, unless mentioned otherwise, all polarization and strains are induced by domain switching and exclude the linear dielectric, piezoelectric and elastic components. The polarization and strain along the poling direction are:

$$P(E) = \frac{48}{4\pi}\int_0^{\pi/4}\mathrm{d}\varphi\int_0^{\operatorname{arccot}(\cos\varphi)} P_0[2(f_{2\text{-}1}z + f_{4-3}x \\ + f_{6-5}y) + f_{4\text{-}1}(z+x) + f_{6\text{-}1}(z+y)]\sin\theta\,\mathrm{d}\theta \quad (19)$$

$$\varepsilon(E) = \frac{48}{4\pi}\int_0^{\pi/4}\mathrm{d}\varphi\int_0^{\operatorname{arccot}(\cos\varphi)} S_0[f_{4\text{-}1}(z^2-x^2) \\ + f_{6\text{-}1}(z^2-y^2)]\sin\theta\,\mathrm{d}\theta. \quad (20)$$

Theoretically, both the polarization and strain can be obtained in closed form as a function of the applied field E but the expression is too long to list. In numerical

studies, Eqs. (19) and (20) are evaluated by using numerical quadrature by dividing the shaded area in Fig. 2 into a 100×100 mesh in the θ and φ directions. The results were found to converge within 0.5% for this mesh size.

Next, consider the case of electric field unloading. It is possible to have 90° back switching during unloading because of the high internal stress. Based on Hwang et al. [13], the 90° switching 4-1 does not cause back switching 1-4 instead to 1-3. Similarly, back switching 1-5 may occur instead of 1-6 in the case of forward switching 6-1. The back-switching criterion depends on the maximum internal stress or maximum achievable 90° switching fraction $f_{4\text{-}1}^{\max}$ and $f_{6\text{-}1}^{\max}$ when the applied field reaches its maximum value $E_{\max}$. The back-switching criterion from 1 to 3 is:

$$E_b[2(f_{4\text{-}1}^{\max} - f_{1-3}) + f_{6\text{-}1}^{\max} - f_{1-5}] - E(z-x) = \sqrt{2}E_C \quad (21)$$

and for 1–5 is:

$$E_b[2(f_{6\text{-}1}^{\max} - f_{1-5}) + f_{4\text{-}1}^{\max} - f_{1-3}] - E(z-y) = \sqrt{2}E_C. \quad (22)$$

Remnant polarization and strain associated with back switching can be expressed as:

$$P(E) = P_{\max} - \frac{48}{4\pi}\int_0^{\pi/4} d\varphi \int_0^{\operatorname{arccot}(\cos\varphi)} P_0[f_{1-3}(z-x) + f_{1-5}(z-y)]\sin\theta\, d\theta \quad (23)$$

$$\varepsilon(E) = \varepsilon_{\max} - \frac{48}{4\pi}\int_0^{\pi/4} d\varphi \int_0^{\operatorname{arccot}(\cos\varphi)} S_0[f_{1-3}(z^2-x^2) + f_{1-5}(z^2-y^2)]\sin\theta\, d\theta, \quad (24)$$

where $P_{\max}$ and $\varepsilon_{\max}$ are the maximum achievable polarization and strain at $E_{\max}$, respectively.

3.1.2. Model B

In the absence of possible 180° switchings 4-3 and 6-5, the switching process of Model B is simpler than that of Model A. Also, the back-switching process of Model B is quite different from that of Model A. The forward 90° switchings 4-1 and 6-1 switch back to their original states (i.e. domains 4 and 6) if back switching occurs.

3.2. Numerical results

Selected numerical results based on the constrained domain-switching model are presented to simulate the poling process of $BaTiO_3$ ceramics [2,8,9]. The material constants used in the simulations are $\mu = 40$ GPa, $v = 0.3$, $P_0 = 26\ \mu C/cm^2$, $S_0 = c/a - 1 = 0.01$, $E_c = 4$ kV/cm. The calculated back electric field, $E_b = 161$ kV/cm. Fig. 4 shows the variation of polarization and strain with the applied electric field for $BaTiO_3$ during electric poling. It can be seen from Fig. 4a that the polarization curve under Model A increases much more rapidly than that under Model B when the electric field exceeds $1.8E_c$. This is because the 180° switching 2-1 is completed at $\sqrt{3}E_C$. When $E > \sqrt{3}E_C$, no unconstrained 180° switching occurs but constrained 90° switching is allowed under Model B, while

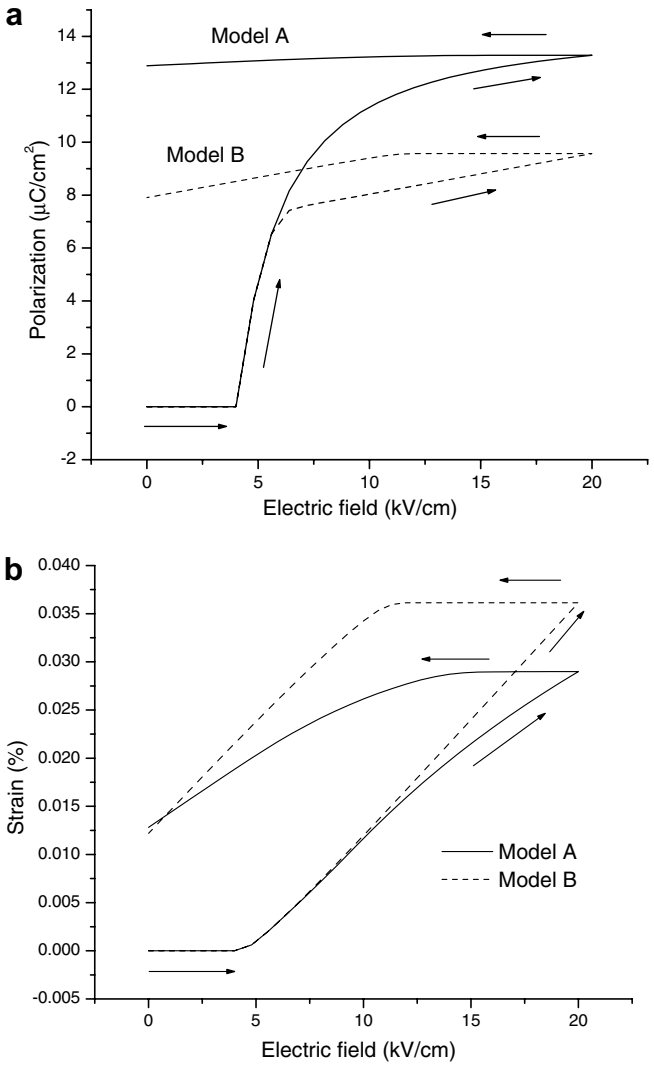

Fig. 4. Polarization and strain of $BaTiO_3$ ceramics during electric poling.

under Model A unconstrained 180° switchings 4-3 and 6-5 coexist. Thus the polarization under Model A is larger than that under Model B for a poling field greater than $\sqrt{3}E_C$. Under Model A, when the poling field reaches $5E_c$, most of the 180° switchings 4-3 and 6-5 can be accomplished. As the polarization by constrained 90° switching is very small (about $0.02P_0$), the remnant polarization approaches the theoretical maximum polarization, $P_0/2$, in the case that complete 180° switching is accomplished without 90° switching [5]. Under Model B, the maximum remnant polarization is the sum of the polarizations by complete 180° switching 2-1 ($0.831/3 = 0.277P_0$) [8] and a small fraction of constrained 90° switching (about $0.02P_0$). In Fig. 4b, although the strain for Model B increases more rapidly than that for Model A when $E > 3E_c$, the remnant strain for both models is not significantly different (about $0.013S_0$).

The main difference between the simulations based on Models A and B is the remnant polarization, which is about $0.5P_0$ for the former and about $0.3P_0$ for the latter.

The measured remnant polarization in $BaTiO_3$ ceramics is about 8 μC/cm^2 ($0.31P_0$) [2] and it appears that Model B can fit the experiments better in the case of $BaTiO_3$. Note that the polarization and strain of tetragonal PZT-45/55 [21,22] was also simulated using experimental material properties and qualitative behavior similar to those of $BaTiO_3$.

The observed domain-switching processes can support the validity of Model B. It has been reported [35,36] that domain switching in ferroelectrics usually starts with nucleation of new domains, followed by domain growth and formation of domain walls, and is finally accomplished via domain wall movement. The energy required for new domain nucleation, domain growth and domain wall formation is usually larger than that for domain wall movement, so once the domain wall is formed, switching via domain wall movement is easier than forming a new domain wall. In Model B, for each type of domain, only one switching path is allowed and it is not allowed to turn to another type of switching during monotonic loading or unloading, which is closer to the real switching process than that under Model A. Furthermore, the switching process under Model B is generally simpler than that under Model A.

The fraction of 90° domain switching in $BaTiO_3$ during electric poling and the remnant fraction of 90° switching after removing the field is shown in Table 1. During electric poling, the 90° switching fraction under Model B is larger than that under Model A especially when the applied field is large. While upon unloading, the remnant 90° switching fractions under the two models are almost the same and increasing the poling field from 3 E_c to 5E_c does not increase the remnant 90° switching fractions. This implies that 3E_c is enough to fully pole a tetragonal ceramic. Note that the calculated remnant 90° switching fraction for $BaTiO_3$ is about 3.3%, which is smaller than the experimental results of 12% by strain measurement [8] and 9% by X-ray diffraction [9]. This implies that the Eshelby inclusion and linear elastic assumptions may overestimate the constraint on 90° switching, and thus underestimate the switching fraction. Further discussion of this aspect is given in Section 5.

4. Constrained domain-switching model for tetragonal ferroelastic ceramics

In tetragonal ferroelastic crystals, there are only three types of domains with their elongation axes along the [100], [010] and [001] directions. Thus it is convenient to redefine the domain types in Fig. 1 by labeling domains 1 and 2 as domain III, domains 3 and 4 as domain I, and domains 5 and 6 as domain II, as shown in Fig. 5. The switching process can be analyzed in a manner similar to the ferroelectric case by using the inverse-pole-figure method and integration over the shaded areas in Fig. 2.

Table 1
Calculated fractions of 90° switching in $BaTiO_3$ ceramic during and after electric poling using the switching options of Models A and B

Loading conditions	Switching options	Fractions (%) of 90° switching
During poling up to 5E_c (or 3E_c)	Model A	6.6 (4.0)
	Model B	11.0 (5.2)
On removing electric field	Model A	3.4 (3.3)
	Model B	3.4 (3.2)

4.1. Model formulation

4.1.1. Model A

Based on Hwang et al. [13], the switching process under uniaxial tension is found to be symmetric to that under uniaxial compression as long as each type of switching is not saturated. It is therefore necessary only to study the switching process under uniaxial compression.

The unpoled state of a ferroelastic ceramic is assumed to be free of internal stress. First consider a ferroelastic grain with the compressive stress σ applied at angles (θ, φ) as shown in Fig. 2. The 90° switchings III–II, III–I and I–II may occur but the switching III–II is preferred over the other two. In fact, only two types of 90° switching can coexist. Following a procedure similar to Section 3.1, it is found that in the case $z^2 + y^2 - 2x^2 > 0$, i.e. $0 < x < 1/\sqrt{3}$, switchings III–II and III–I may coexist. Otherwise, i.e. $1/\sqrt{3} < x < 1/\sqrt{2}$, switchings III–II and I–II may coexist. For convenience, the shaded area in Fig. 2 is cut to two parts by the plane $x = 1/\sqrt{3}$ with the back part $(0 < x < 1/\sqrt{3})$ labeled as S_1 and the front part $(1/\sqrt{3} < x < 1/\sqrt{2})$ as S_2.

Now consider the switching III–II at S_1 to present a 90° domain-switching criterion. The following relationship is analogous to Eq. (11):

$$\Delta f_{\text{III–II}}\sigma S_0(z^2 - y^2) - \Delta f_{\text{III–II}} \cdot 2\mu \frac{7 - 5v}{15(1 - v)} S_0^2 (2f_{\text{III–II}} + f_{\text{III–I}}) \geqslant \Delta f_{\text{III–II}} \cdot W_{90}^{\sigma}, \tag{25}$$

where W_{90}^{σ} is the energy barrier (per unit volume) for 90° switching under mechanical loading.

It is assumed that $W_{90}^{\sigma} = \sigma_C S_0$ to activate 90° switching when the applied stress reaches the coercive stress σ_c. By dividing both sides of Eq. (25) by $\Delta f_{\text{III–II}} S_0$ and introducing $\sigma_b = 2\mu \frac{7-5v}{15(1-v)} S_0$, Eq. (25) can be expressed as:

$$\sigma(z^2 - y^2) - \sigma_b \cdot (2f_{\text{III–II}} + f_{\text{III–I}}) = \sigma_C, \tag{26}$$

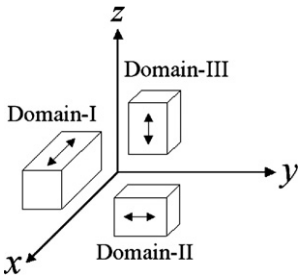

Fig. 5. Three types of domain in tetragonal ferroelastic crystals.

where σ_b is an equivalent resisting stress induced by 90° switching, analogous to E_b. It can be called the "back stress".

In the case that switchings III–II and III–I coexist, the switching criterion for III–I is:

$$\sigma(z^2 - x^2) - \sigma_b \cdot (f_{III-II} + 2f_{III-I}) = \sigma_C. \quad (27)$$

By solving Eqs. (26) and (27), the fraction of 90° switching can be explicitly obtained as a function of the applied stress σ and the two Eulerian angles (θ, φ). The strain induced by switching can be expressed in terms of area integrals similar to Eq. (20).

4.1.2. Model B

Based on Berlincourt and Krueger's switching option under electric loading [8], Model B can be extended to the ferroelastic case such that during uniaxial compression (tension) loading, domains are only allowed to switch to the state with its elongation axis furthest (closest) to the compression (tension) loading direction. That is, there only exist 90° switchings III–II and I–II during compression while only switchings II–III and I–III exist during tension. The analysis of the switching process is similar to but simpler than that of Model A and is therefore not discussed here.

4.2. Numerical results

Fig. 6 shows the stress–strain curves of $BaTiO_3$ ceramics subjected to uniaxial compression (tension) up to $5\sigma_c$ using Models A and B. In addition to the previously mentioned material constants, $W_{90}^{\sigma} = W_{90}^{E}$ is used. Therefore, $\sigma_C = \sqrt{2}P_0E_C/S_0 = 14.7$ MPa. The calculated σ_b is 419 MPa. It can be seen that under uniaxial tension, there is little difference between the stress–strain curves corresponding to Models A and B, although the latter forbids some possible 90° switching from II to I when a field is applied to S_2. This is because the area of S_2 is only $(2-\sqrt{3})/1 = 27\%$ of the shaded area in Fig. 2. The switching strain by the secondary 90° switching II–I on such a small area is almost negligible. However, for uniaxial compression, the switching-induced strain under Model A is slightly larger than that under Model B because the latter forbids some possible 90° switching from III to I when a field is applied to S_1, which is 73% of the shaded area in Fig. 2. Remnant strains corresponding to the two models show little difference.

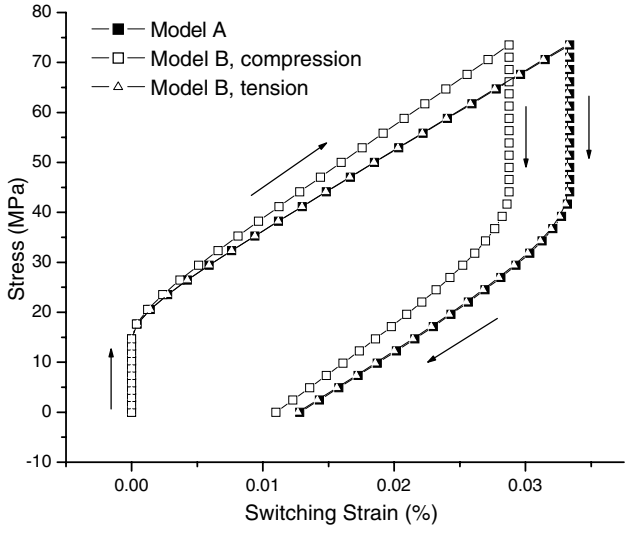

Fig. 6. Stress–strain curves of $BaTiO_3$ ceramics under uniaxial compression (tension).

5. Discussion

The proposed constrained domain-switching model shows that in $BaTiO_3$ ceramics, only 3-4% of remnant 90° domain switching can be achieved during electric poling and the fraction is no more than 10% during mechanical loading, which agrees well with the existing experimental results [8,9]. From the present analysis, it can be seen that the fraction of achievable 90° switching is strongly dependent on the back electric field, E_b, which is proportional to S_0^2/P_0 during electric loading, and on the back stress, σ_b, which is proportional to S_0 during mechanical loading. The larger the E_b (or σ_b) is, the smaller the fraction of 90° switching that can be achieved during electric (or mechanical) loading. The achievable fraction of 90° switching, f_{90}, during loading for Model B can be estimated by the following formulae when f_{90} is not very large (say less than 20%):

$$f_{90} \approx \begin{cases} (E_{max} - E_C)/E_b & \text{for electric loading} \\ (\sigma_{max} - \sigma_C)/\sigma_b & \text{for mechanical loading} \end{cases}. \quad (28)$$

For $BaTiO_3$ ceramics, the ratio E_b/E_c is about 40, which leads to $f_{90} = 10\%$ at $5E_c$ when compared to the calculated value of 11% shown in Table 1. The ratio σ_b/σ_c is 28.5 and the estimated f_{90} is 14% at $5\sigma_c$, only slightly smaller than the simulated value of 15%.

It should be noted that in $BaTiO_3$ ceramics, the calculated fraction of achievable 90° switching, which is 11% during electric poling up to $5E_c$ (20 kV/cm) and 3.4% upon removing the field, is smaller than the experimental results of 17% and 12% (or 10%) [8,9], respectively. This difference is probably because the present model, which is based on linear elasticity and considers the internal stress induced by non-180° switching in an Eshelby inclusion manner with the assumption of an infinite matrix, is limited to situations where f_{90} is relatively small. In the case that f_{90} is relatively large (say >10%), the constraint by neighboring grains is reduced and the model slightly overestimates the internal stress, thus underestimating f_{90} during electric (mechanical) loading and overestimating it during back switching upon removing the field. Another point to note is that in a real ferroelectric ceramic, during the holding time of poling field, internal stresses relax and an internal bias field [37] may build up in the material, both of which help to stabilize the switched domains and resist reversal of non-180° switching on removing the poling field.

6. Conclusions

A constrained domain-switching model is proposed for polycrystalline ferroelectric/ferroelastic ceramics that are made up of multi-domain grains. The model takes into account the charge-screening effect in real ceramics and considers the internal stress induced by non-180° switching in an Eshelby inclusion manner. Thus non-180° switching is constrained by neighboring grains while 180° switching is not constrained at all. The model is based on a potential energy-dependent domain-switching criterion and uses switching options based on the models of either Hwang et al. [13] or Berlincourt and Krueger [8]. Numerical simulations show that solutions obtained using Berlincourt and Krueger's switching option agree better with experiments. It is found that only a few per cent of 90° switching can occur in $BaTiO_3$ and tetragonal PZT ceramics for up to five times the coercive electric (stress) field, which agrees well with the existing experimental results [8,9,20–22]. In addition, the inverse-pole-figure method used in this paper, which fixes the crystallite coordinates and varies the field direction, is an effective approach for analyzing the constitutive behavior of polycrystalline materials under vector loading (such as electric or magnetic loading, etc.) or uniaxial compression (tension). To the best of our knowledge, the current model is the first attempt to predict the fraction of 90° (or non-180°) switching without any fitting parameters. The model can be extended to include all possible co-switching of 90° domains and rhombohedral ceramics as shown in a subsequent paper [23].

Acknowledgements

The work presented in this paper was supported by a grant from the Natural Sciences and Engineering Research Council of Canada (NSERC).

References

[1] Xu Y. Ferroelectric materials and their applications. Amsterdam: North-Holland; 1991.
[2] Jaffe B, Cook WR, Jaffe H. Piezoelectric ceramics. London/New York: Academic Press; 1971.
[3] Baerwald HG. Phys Rev 1957;105:480.
[4] Redin RD, Marks GW, Antoniak CE. J Appl Phys 1963;34:600.
[5] Li FX, Rajapakse RKND. J Appl Phys 2007;101:054110.
[6] Landis CM. J Appl Mech – T ASME 2003;70:470.
[7] Li FX, Fang DN, Soh AK. Scripta Mater 2006;54:1241.
[8] Berlincourt D, Krueger HHA. J Appl Phys 1959;30:1804.
[9] Subbarao EC, McQuarrie MC, Buessem WR. J Appl Phys 1957;28:1194.
[10] Zhang XW, Lei C, Chen KP. J Am Ceram Soc 2005;88:335.
[11] Kamlah M, Tsakmakis C. Int J Solids Struct 1999;36:669.
[12] Landis CM. J Mech Phys Solids 2002;50:127.
[13] Hwang SC, Lynch CS, McMeeking RM. Acta Metall Mater 1995;43:2073.
[14] Hwang SC, Huber JE, McMeeking RM, Fleck NA. J Appl Phys 1998;83:1530.
[15] Huber JE, Fleck NA, Landis CM, McMeeking RM. J Mech Phys Solids 1999;47:1663.
[16] Zeng X, Rajapakse RKND. Acta Mater 2003;51:4121.
[17] Li FX, Fang DN. Mech Mater 2004;36:959.
[18] Kamlah M, Liskowsky AC, McMeeking RM, Balke H. Int J Solid Struct 2005;42:2949.
[19] Wan S, Bowman KJ. J Mater Res 2001;16:2306.
[20] Li JY, Rogan RC, Üstündag E, Bhattacharya K. Nature Mater 2005;4:776.
[21] Hoffmann MJ, Hammer M, Endriss A, Lupascu DC. Acta Mater 2001;49:1301.
[22] Lupascu DC. Fatigue in ferroelectric ceramics and related issues. Berlin/New York: Springer Verlag; 2004.
[23] Li FX, Rajapakse RKND. Acta Mater 2007;55:6481. doi:10.1016/j.actamat.2007.08.003.
[24] Hall DA, Steuwer A, Cherdhirunkorn B, Withers PJ, Mori T. J Mech Phys Solids 2005;53:249.
[25] Lines ME, Glass AM. Principles and applications of ferroelectrics and related materials. Oxford: Clarendon Press; 1977. p. 87.
[26] Lehovec K. J Chem Phys 1953;21:1123.
[27] Käenzig W. Phys Rev 1955;98:549.
[28] Mehta K, Virkar AV. J Am Ceram Soc 1990;73:567.
[29] Taylor GI. J Inst Met 1938;62:307.
[30] Bhattacharya K, Kohn RV. Acta Mater 1996;44:529.
[31] Eshelby JD. Proc R Soc A 1957;241:376.
[32] Mura T. Micromechanics of defects in solids. London: Martinus Nijhoff; 1982. p. 67.
[33] Bunge HJ. Texture analysis in materials science. Berlin: Butterworth; 1982.
[34] Hill R. The mathematical theory of plasticity. Oxford: Clarendon Press; 1950.
[35] Merz WJ. Phys Rev 1954;95:690.
[36] Lente MH, Eiras JA. J Appl Phys 2001;89:5093.
[37] Takahashi S. Ferroelectrics 1982;41:143.